December 5th, 2012

An overview of optical communication for deep space: issues, challenges, solutions

by

Baris I. Erkmen, Bruce E. Moision, and Samuel J. Dolinar

Jet Propulsion Laboratory, California Institute of Technology

Deep-space optical communication

- Why optical communications to, from, in space?
- Optical communication systems
  - system diagram, link equations, fundamental capacity bounds
- Impairments to the optical channel
  - atmosphere-induced losses
  - pointing-induced losses
  - receiver-induced losses
- Conclusions

Why optical communication?

- Ever-growing demand for data rate and data volume
  - increase in science return from interplanetary missions
  - increasing desire for connectivity via high-bandwidth links

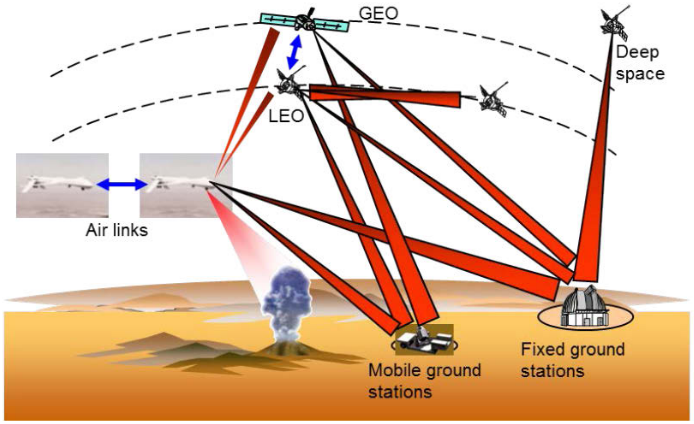

- Optical frequencies much higher in the EM spectrum than radio frequencies
  - higher carrier frequency: smaller diffraction of transmitted beams
  - unallocated spectrum: significantly higher modulation bandwidth

Radio frequency (RF) versus optical links

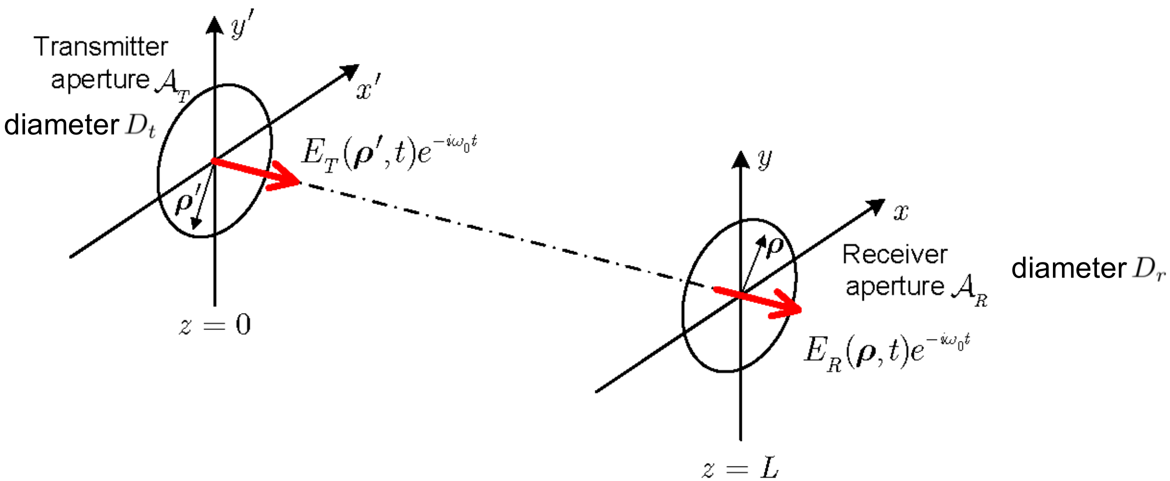

representative RF and optical links

(r)	Ka-band Link	
f	carrier frequency	32.0 GHz
D_t	transmit diameter	3.0 m
D_r	receiver diameter	34.0 m
η	system efficiency	-10.88 dB
N_o	noise spectral density	-178.45 dB-mW/Hz
W	bandwidth	500 MHz
P_t	transmit power	35 W

(o)	Near-Infrared Link	
λ	wavelength	1.55 μm
D_t	transmit diameter	22.0 cm
D_r	receiver diameter	11.8 m
η	system efficiency	-16.74 dB
α_b	noise spatial density	1.0 pW/m^2
T_s	slot width	0.5 ns
P_t	transmit power	4 W

- At optical-frequency links
  - I. diffraction loss is significantly smaller than RF
  - II. nominal aperture sizes are smaller
  - III. photon energy is significantly higher → more noise per photon
  - IV. nominal transmitter and receiver efficiencies are lower

fractional power coupling of optical links higher

$$\frac{C_{\mathrm{OPT}}}{C_{\mathrm{RF}}} = \left(\frac{\lambda^{(\mathrm{r})}}{\lambda^{(\mathrm{o})}}\right)^2 \left(\frac{D_t^{(\mathrm{o})} D_r^{(\mathrm{o})}}{D_t^{(\mathrm{r})} D_r^{(\mathrm{r})}}\right)^2 \left(\frac{N_0^{(\mathrm{r})}}{(hc/\lambda^{(\mathrm{o})})/\log_2 M}\right) \left(\frac{\eta^{(\mathrm{o})}}{\eta^{(\mathrm{r})}}\right)$$

I. +76 dB

II. -33 dB

III. -12 dB

IV. -16 dB

net = +15 dB

Channel impairments in free-space optical links

- The link design must overcome channel impairments
- Atmosphere-induced impairments:
  - absorption: atmospheric extinction
  - turbulence: scintillation, beam spread and angle-of-arrival spread
- Pointing-induced impairments:
  - time-dependent fluctuations in power delivered to receiver
- Receiver-induced impairments:
  - shot noise
  - background radiation noise
  - photodetector impairments: blocking, timing jitter, nonlinear responsivity
  - post-detection electronic noise

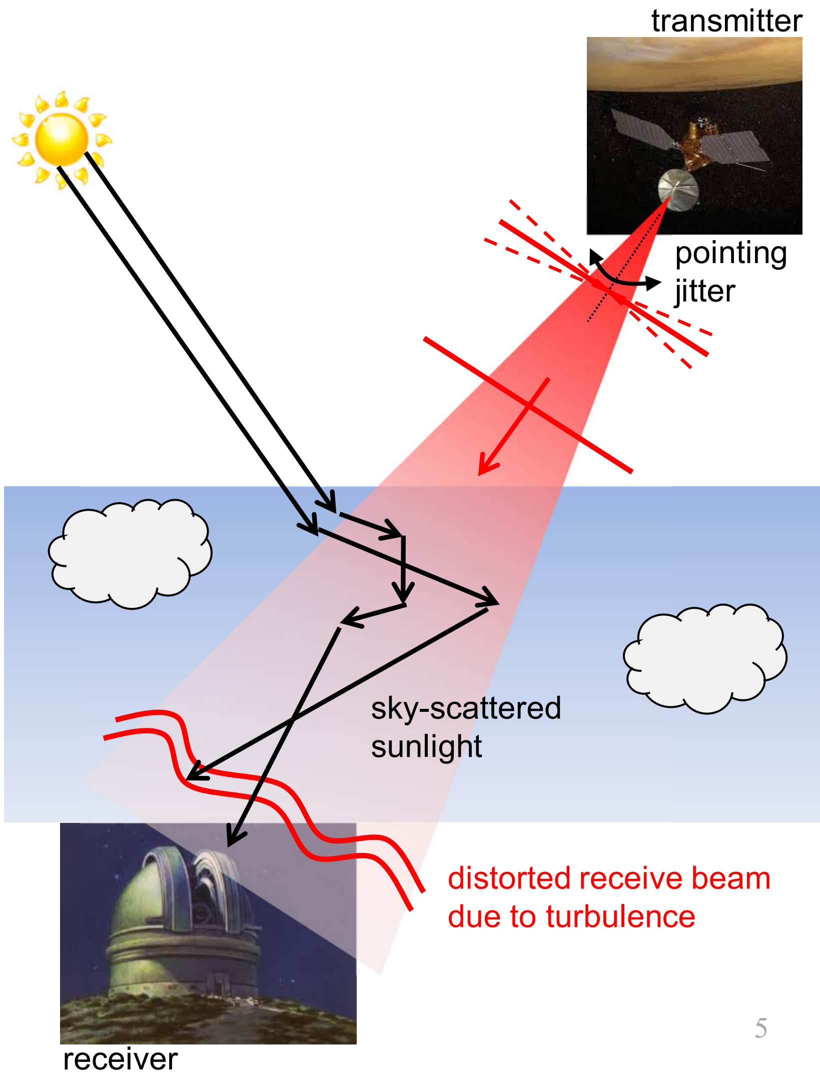

End-to-end system diagram

- The overall system performance depends on
  - modulation method and detection method
  - pointing, acquisition and tracking performance (both flight and ground)
  - transmitter resources (e.g., photon flux)
  - channel code performance

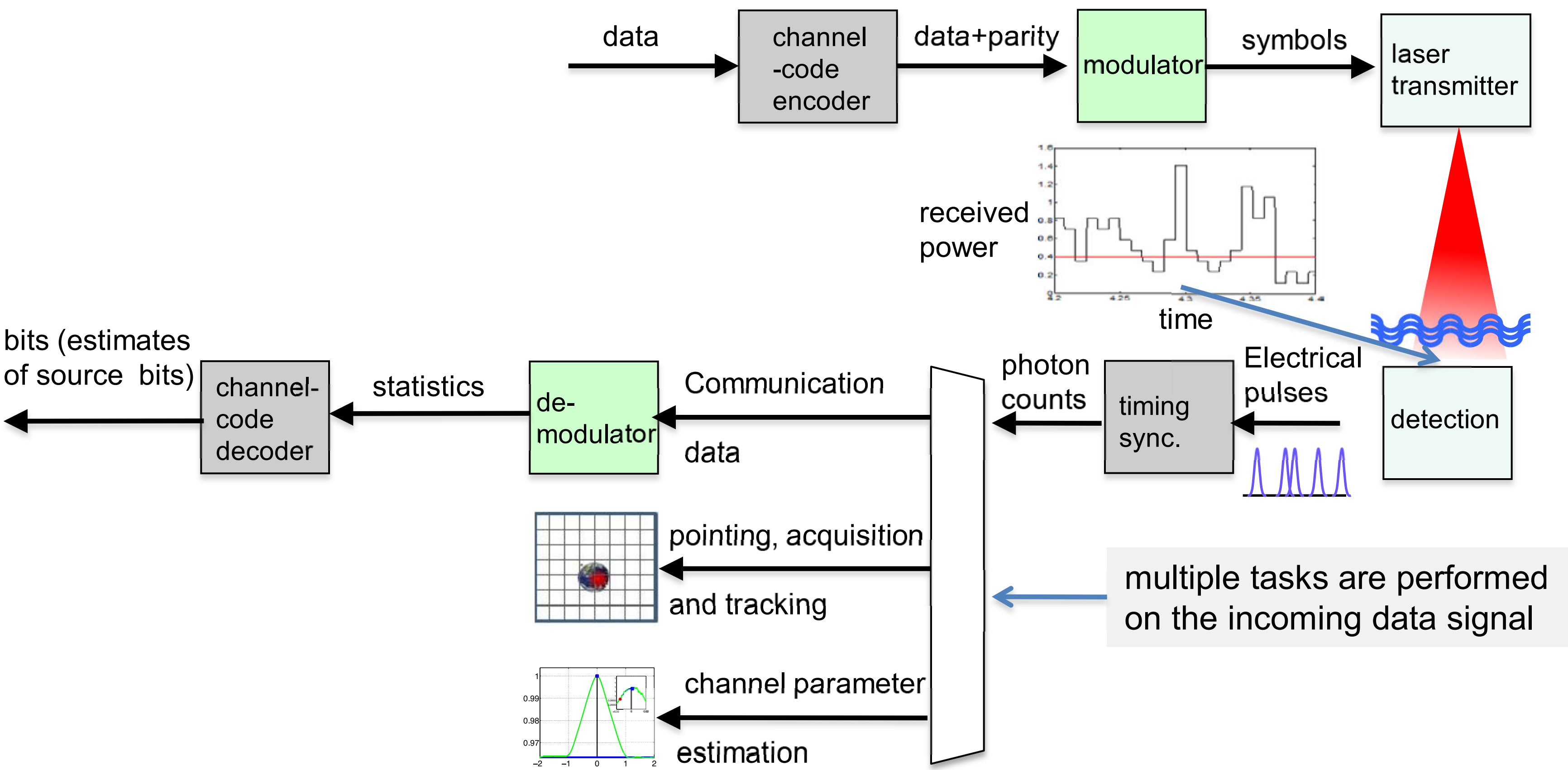

Link performance evaluation

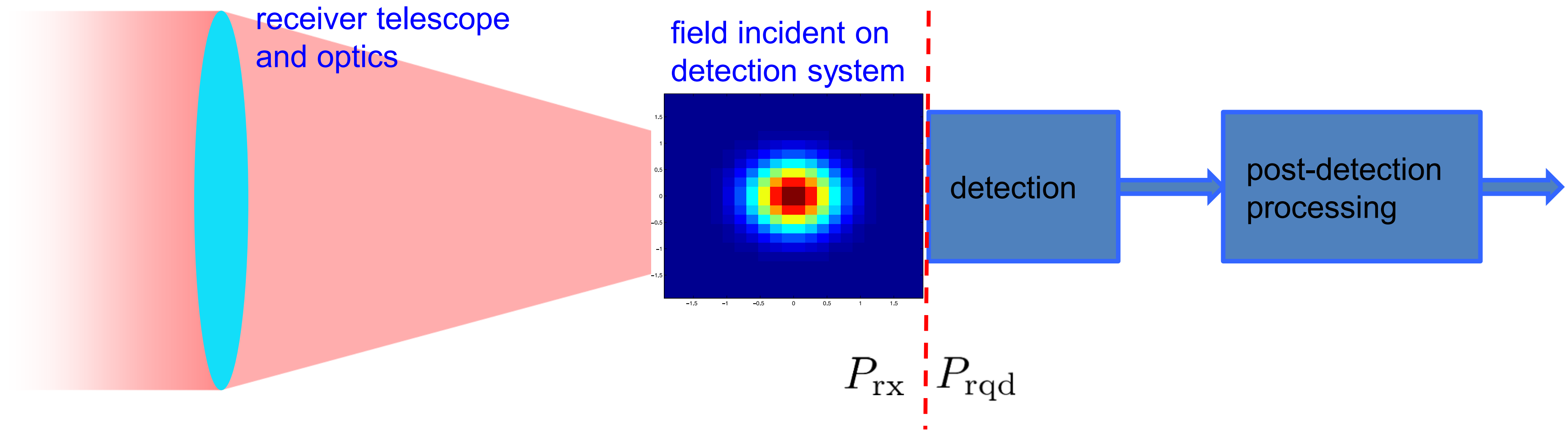

$$P_{\mathrm{rx}} = P_t G_t G_r L_s L_a \eta_{\mathrm{pt}} \eta_t \eta_r$$

- Power incident on the detection subsystem
  - P_t : transmitted power
  - $G_t,\ G_r$: transmit & receive aperture gains
  - L_s : space loss
  - L_a : atmospheric loss
  - η_{pt} : pointing loss
  - $\eta_t,\ \eta_r$: transmit & receive efficiencies

$$P_{\mathrm{rqd}} = P_i / (L_b L_j L_f L_t \eta_{\mathrm{det}} \eta_{\mathrm{imp}} \eta_{\mathrm{code}} \eta_{\mathrm{int}})$$

- required signal power to support target data rate
  - P_i : minimum (ideal receiver) required power
  - $L_b,\ L_j,\ \eta_{\mathrm{det}}$: detector blocking, jitter & efficiency losses
  - L_f : fading loss
  - L_t : truncation loss (angle-of-arrival spread)
  - η_{imp} : implementation efficiency
  - $\eta_{\mathrm{code}}, \eta_{\mathrm{int}}$: code & interleaver efficiencies

Link margin [dB] $= 10 \log_{10}(P_{\mathrm{rx}}/P_{\mathrm{rqd}})$

Conventional detection methods

- Direct detection:
  - measures photon-flux of incident field
  - ideal limit yields Poisson statistics with rate equal to incident photon flux

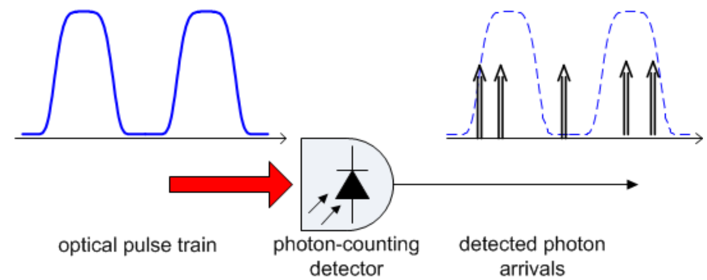

- Heterodyne detection:
  - measures real and imaginary quadratures of field
  - ideal limit yields Gaussian statistics with mean equal to incident field amplitude and variance ½ per dimension.

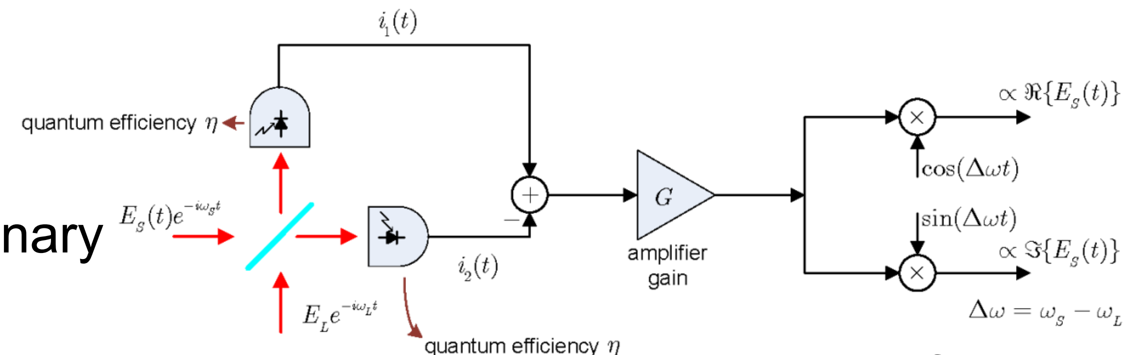

- Homodyne detection:
  - measures Real quadrature of field
  - ideal limit yields Gaussian statistics with mean equal to quadrature of incident field and variance ¼.

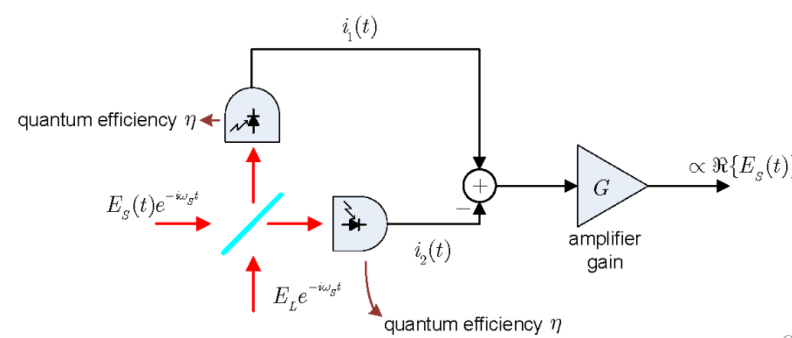

Coherent versus incoherent detection

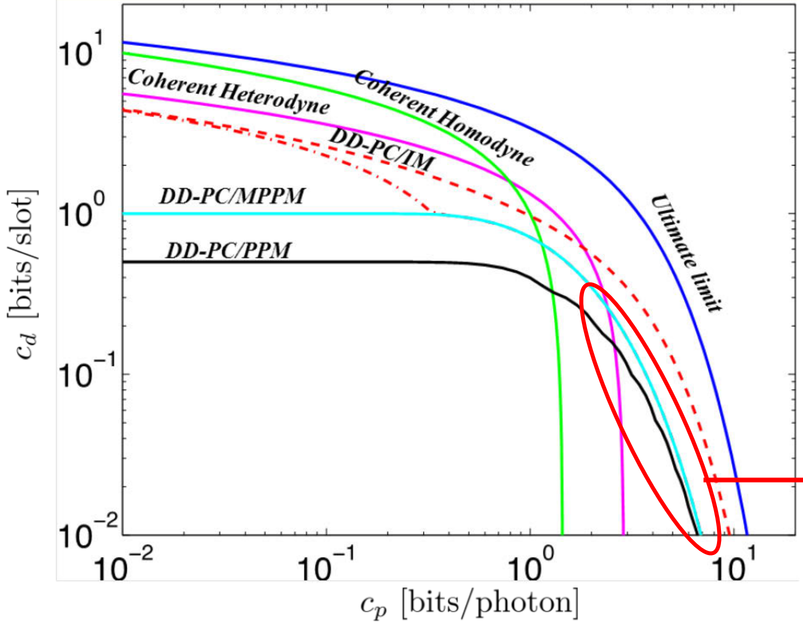

DD: direct detection
PC: photon-counting (ideal)
PPM: Pulse-position modulation
MPPM: Multipulse PPM
IM: Intensity modulation

regime of interest for deep-space links

- Resource efficiency curves obtained via information theory
  - *Photon efficiency* (c_p): capacity [bits/s] / average photon flux [photons/s]
  - *Bandwidth efficiency* (c_d): capacity [bits/s] / modulation bandwidth [1/s]
- Direct detection receivers + binary intensity modulations asymptotically optimal in photon efficiency
- Heterodyne and homodyne receivers + coherent-state modulations encounter brick-wall asymptotes in photon efficiency

Binary intensity modulation and photon-counting

- To achieve high photon efficiency, average photon number per channel use must be *low*
  - binary modulation alphabet is near-optimal: often transmit nothing, send a pulse sparsely
  - results in low duty cycle $\Rightarrow$ high peak-to-average photon flux

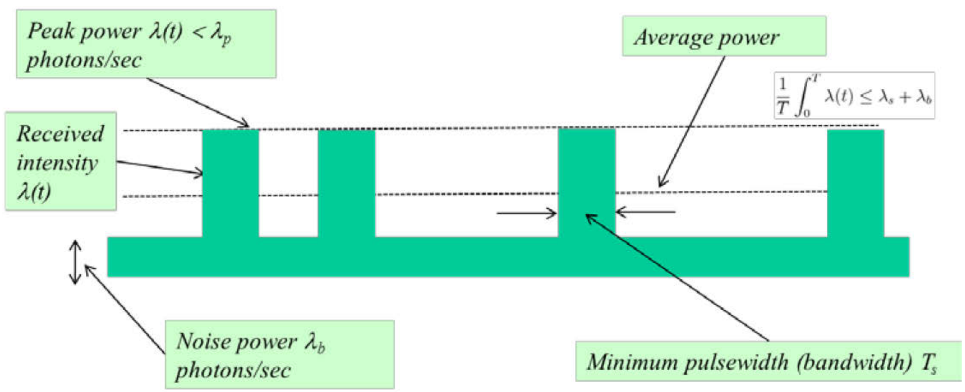

On-Off-Keying (OOK): 1 bit is represented by a slot, which may either be occupied by a pulse or not

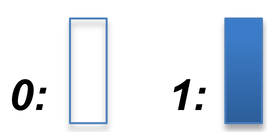

Pulse-Position-Modulation (PPM): $log_2 M$ bits are represented by a single pulse out of *M* slots *(here M=16).*

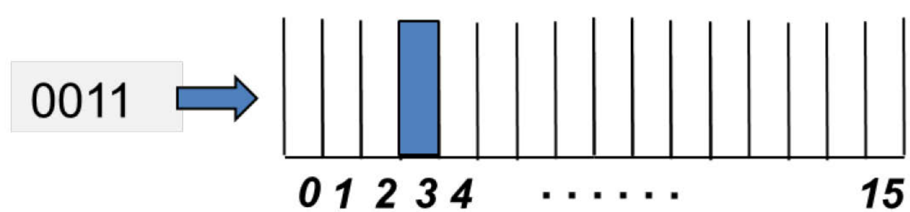

Photon-counting statistics

- Ideal photon-counting yields photon arrivals as a Poisson point process with rate function proportional to incident photon flux

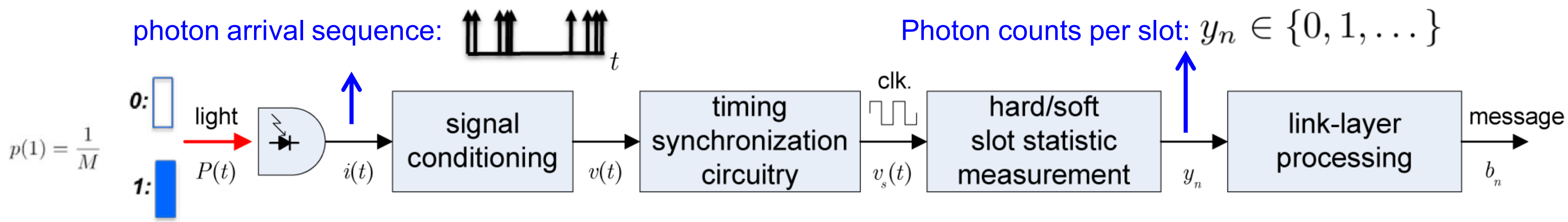

- After synchronization an equivalent discrete channel can be defined

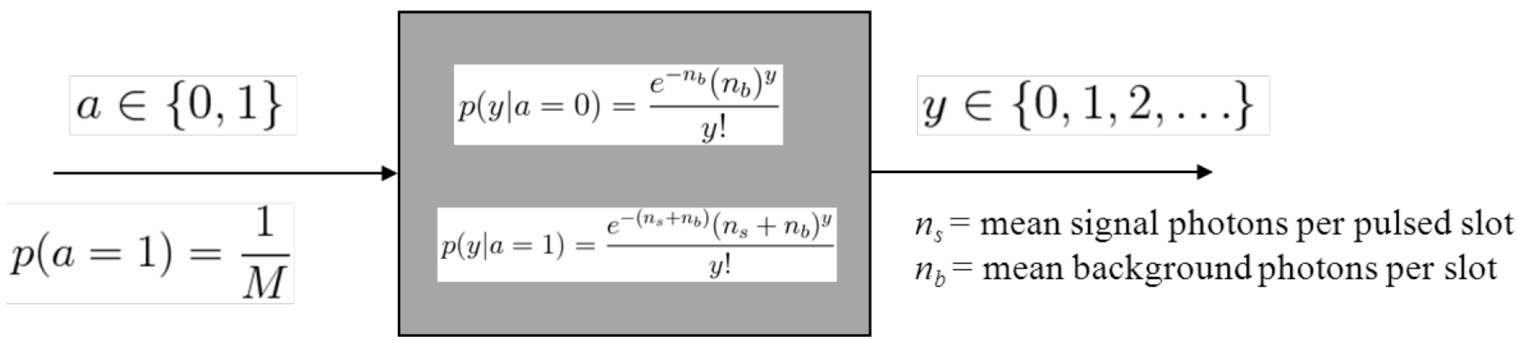

A simple example for reliable information transfer

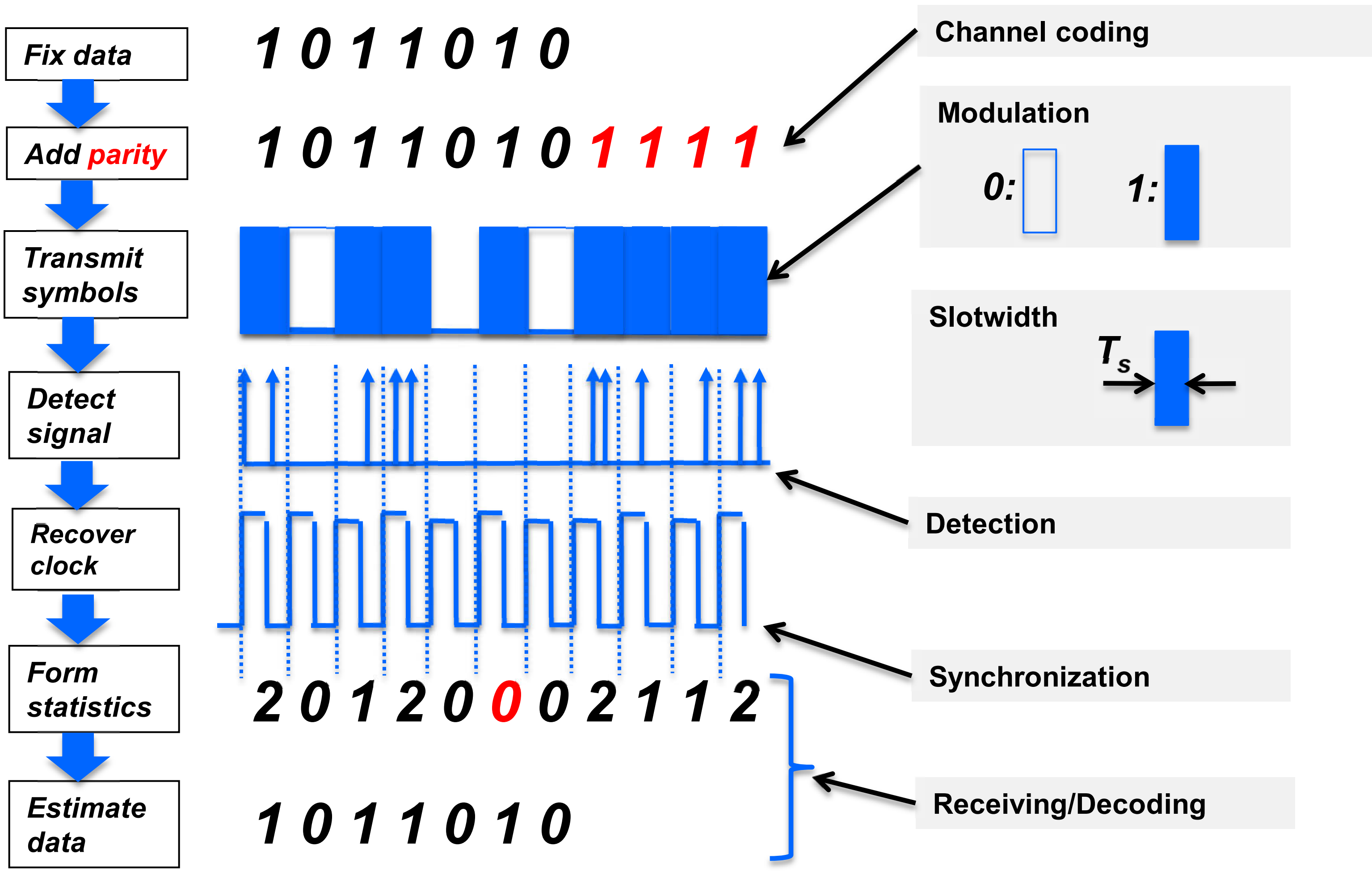

Optimal processing of photon counts

- Deciding on each bit independently (based on photon counts in the slot) is suboptimal

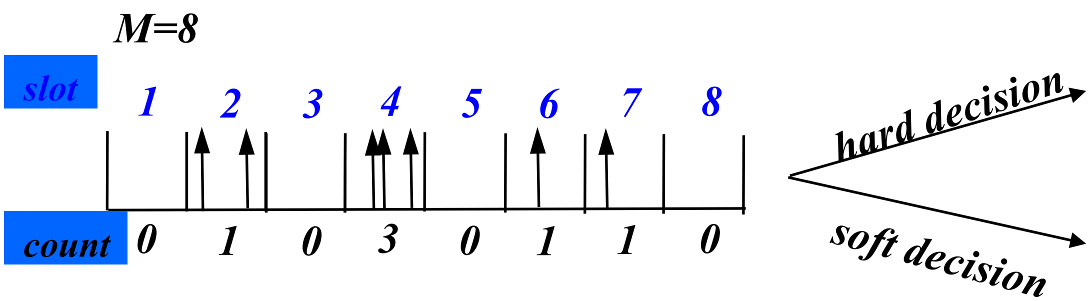

$\hat{x} = 011$

p(x=000|y) = 0.05
p(x=001|y) = 0.2
p(x=010|y) = 0.05
p(x=011|y) = 0.3
…

- Photon-number gap is several dB between hard and soft decisions

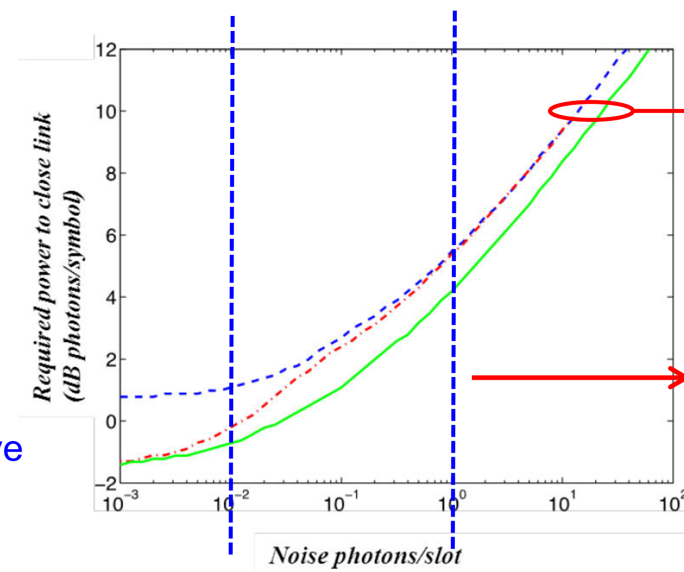

hard decisions
hard decisions with erasures
soft decisions

typical region of operation is between 0.01 and 1.0 photons/slot

average power required to achieve C = 1/8 bits/slot for M=16 slots

Channel impairments:
I. Atmospheric effects

Optical communication through the atmosphere

- Atmospheric layer mostly concentrated in 0-20km above ground, although it extends up to 100km
- Atmospheric effects on performance:
  - bad weather (e.g., snow, fog, rain), and particulates cause absorption and scattering

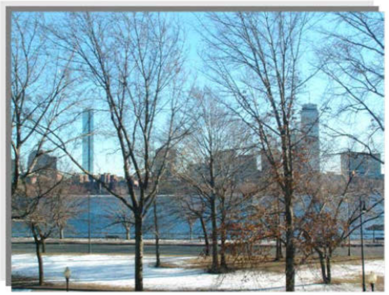

  - in clear weather *turbulence* causes fading, beam and angular spread

- Impact in Earth-space links are *asymmetric*

Loss due to atmospheric extinction

- Absorption and scattering from aerosols (dust, etc.) and molecules (water vapor, etc.) attenuate the signal
- In bad weather (rain, snow, fog), attenuation can be severe, causing dropouts
- Even in *clear-sky* conditions must budget for attenuation
  - Drives selection of bands with good clear-sky transmissivity
- Typical attenuation for Earth-space link in near-infrared at zenith 0.1 -- 0.3 dB

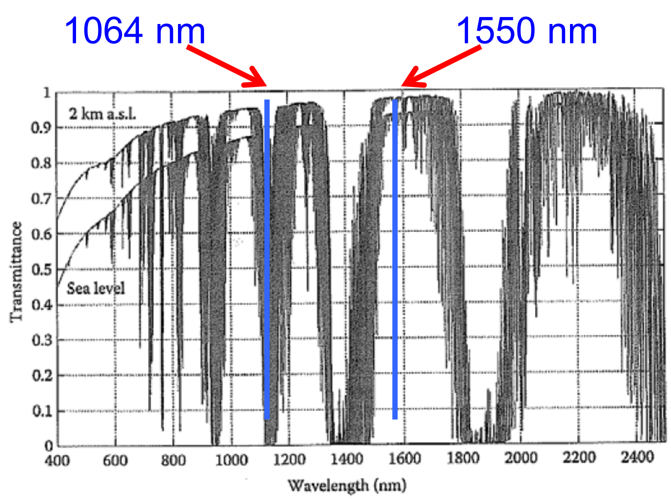

FIGURE 8.12 Atmospheric transmittance in an Earth-to-space path at zenith. A rural aerosol composition with a surface visual range of 23 km is considered. The data refers to the case of an observer located at two elevations: sea level (lower transmittance) and 2 km above sea level.

Piazzolla, Near-Earth Laser Communications 2009

Clear-air turbulence effects

- Random spatio-temporal mixing of air with different temperatures causes refractive-index variations
  - scintillation (constructive/destructive interference)
  - angle-of-arrival variations
  - beam spreading
  - beam wander

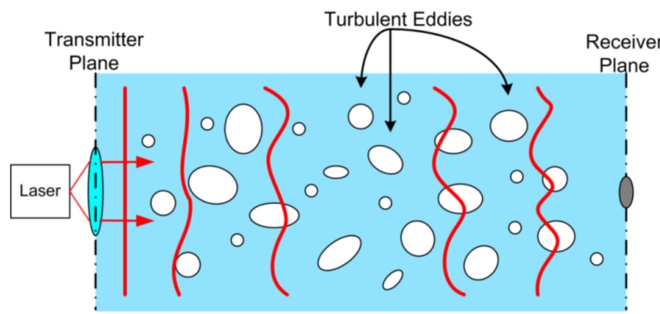

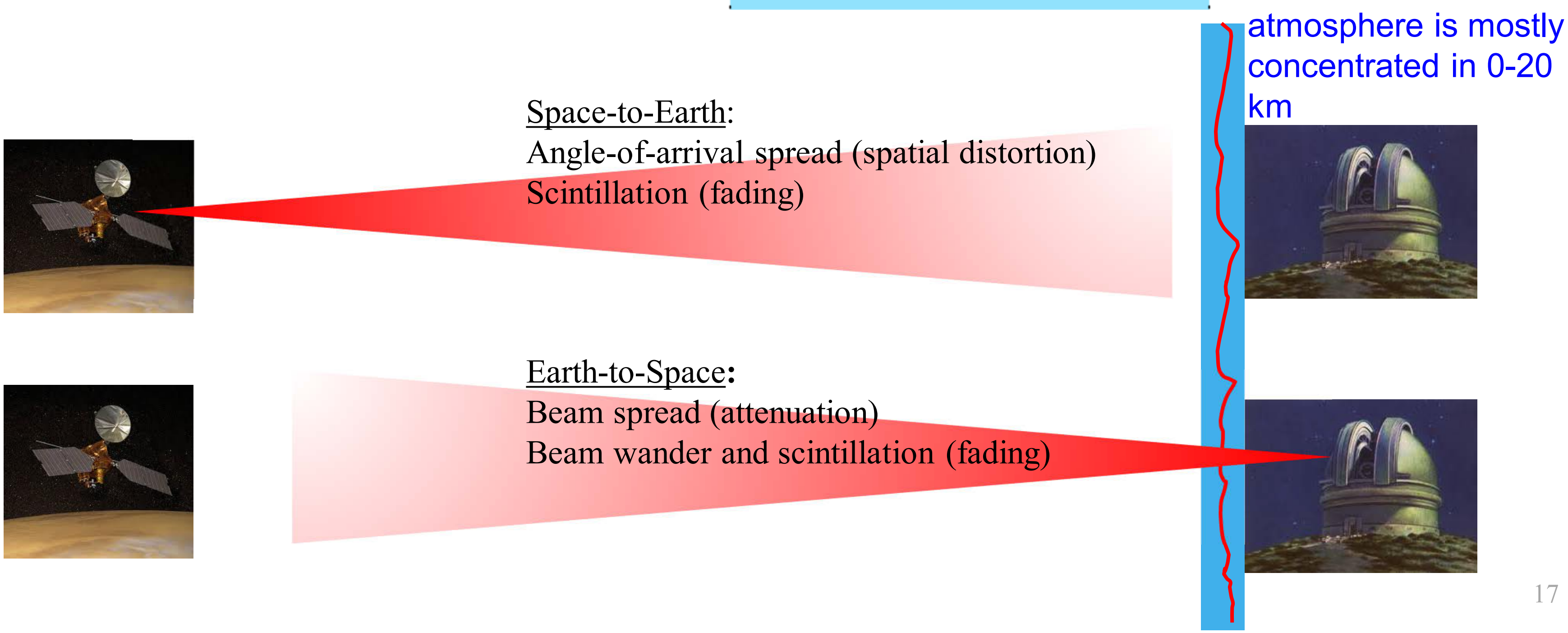

Impact on downlink

- Extended Huygens-Fresnel principle models paraxial quasimonochromatic propagation through turbulence

transfer function from aperture to focal plane

$$E_f(\boldsymbol{\rho}) = \int \mathrm{d}\boldsymbol{\rho}' E_r(\boldsymbol{\rho}') e^{\chi(\boldsymbol{\rho}') + i\phi(\boldsymbol{\rho}')} h_f(\boldsymbol{\rho}, \boldsymbol{\rho}')$$

jointly Gaussian random fields having

$$\langle e^{\chi(\boldsymbol{\rho}_1) - i\phi(\boldsymbol{\rho}_1)} e^{\chi(\boldsymbol{\rho}_2) + i\phi(\boldsymbol{\rho}_2)} \rangle = e^{-D(\boldsymbol{\rho}_2 - \boldsymbol{\rho}_1)/2}$$

$$D(\boldsymbol{\rho}) = |\boldsymbol{\rho}|^{5/3} / r_0^{5/3}$$ receiver-plane coherence length

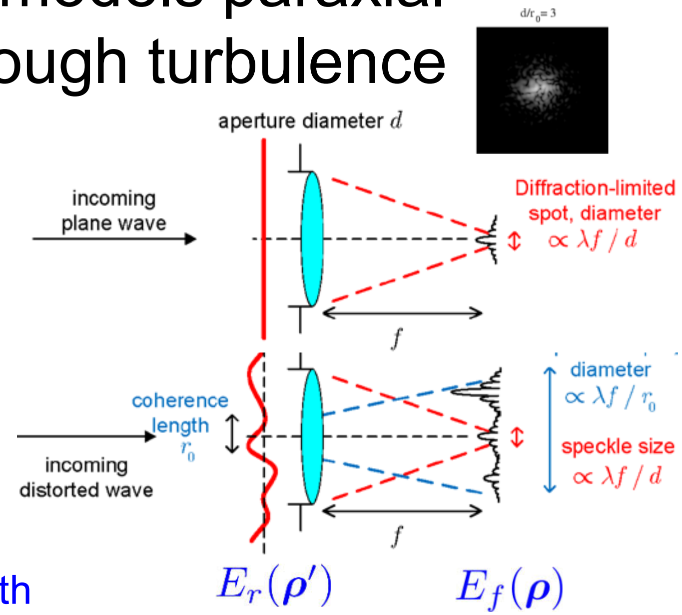

- Field incident on the photodetector plane has speckle
  - short-exposure brightest spot will wander on the photodetector surface
  - long-exposure average will be broader than diffraction limit
- To accommodate angle-of-arrival fluctuations, field-of-view of detector larger than vacuum $\Rightarrow$ increase in background

Impact on uplink

- Extended Huygens-Fresnel principle yields

vacuum-propagation Green's function

$$E_r(\boldsymbol{\rho}) = \int \mathrm{d}\boldsymbol{\rho}' E_t(\boldsymbol{\rho}') e^{\chi(\boldsymbol{\rho}')+i\phi(\boldsymbol{\rho}')} h_{\mathrm{fs}}(\boldsymbol{\rho}-\boldsymbol{\rho}';L)$$

jointly Gaussian random fields having

$$\langle e^{\chi(\boldsymbol{\rho}_1)-i\phi(\boldsymbol{\rho}_1)} e^{\chi(\boldsymbol{\rho}_2)+i\phi(\boldsymbol{\rho}_2)}\rangle = e^{-D(\boldsymbol{\rho}_2-\boldsymbol{\rho}_1)/2}$$

$$D(\boldsymbol{\rho}) = |\boldsymbol{\rho}|^{5/3}/r_0^{5/3} \longrightarrow$$ transmitter-plane-coherence length

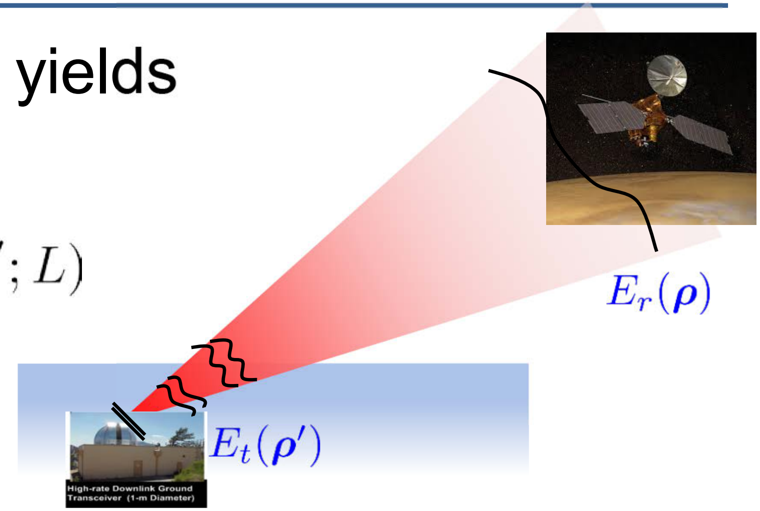

- Taylor-series expanding phase term shows various effects
  - $\phi_2(\boldsymbol{\rho})$: short-term beam spread (relative to vacuum propagation)
  - $\boldsymbol{k}_0$: beam wander (randomly-varying tilt at transmitter plane)
  - $\chi(\boldsymbol{\rho})$: scintillation

$$\phi(\boldsymbol{\rho}) = \phi_0 + \boldsymbol{\rho}\cdot\boldsymbol{k}_0 + \phi_2(\boldsymbol{\rho})$$

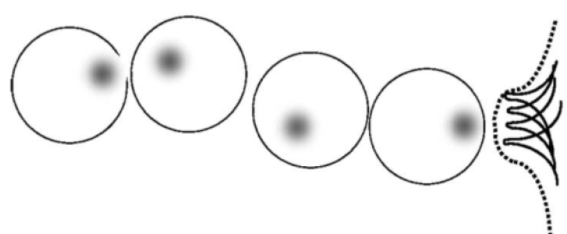

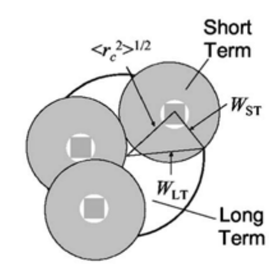

Andrews & Phillips, Laser Beam Propagation Through Random Media, 2006

Time-dependent power fluctuations

- Turbulence causes the incident photon flux to fluctuate

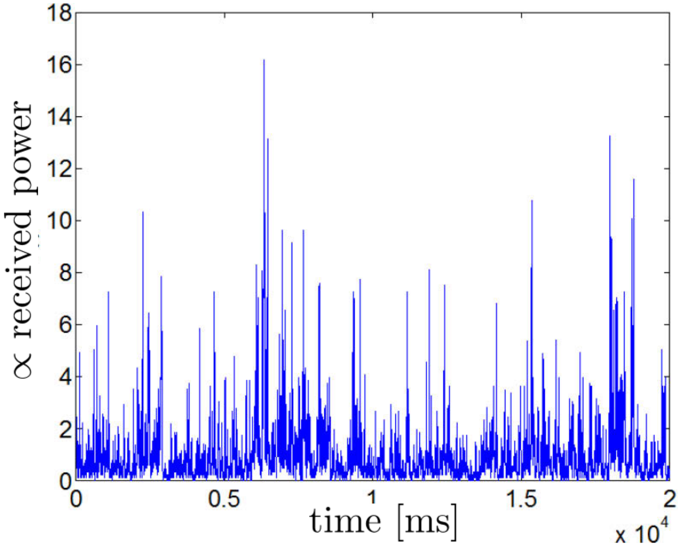

Biswas & Wright, Measured fluctuations over a 45-km mountain-top to mountain-top link, 2002

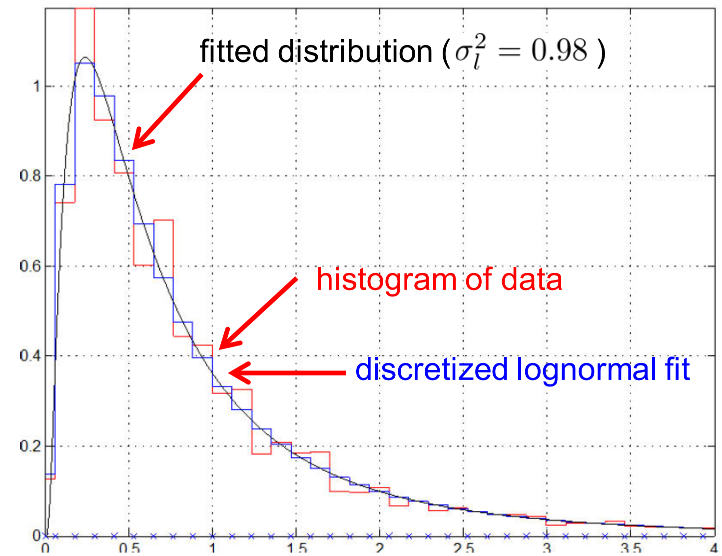

- Fluctuations in weak turbulence are often well-modeled as log-normally distributed $P_r(t) = P_0 V(t)$

$\langle V(t) \rangle = 1$

marginal distribution: $$f_V(v) = \frac{1}{\sqrt{2\pi\sigma_l^2}} \frac{1}{v} \exp\left(\frac{-(\log v + \sigma_l^2/2)^2}{2\sigma_l^2} \right)$$

Block fading model for photon-flux fluctuations

- $P_r(t)$ exhibits a coherence time on the order of ~msec

- We define coherence time as inverse of 90% bandwidth

$$W(\xi) \equiv \left\{ B : \int_{-B}^{B} \mathrm{d}f\, S_x(f) \Big/ \int_{-\infty}^{\infty} \mathrm{d}f\, S_x(f) = \xi \right\}$$

$$T_{\text{coh}} \equiv \frac{1}{W(0.9)}$$

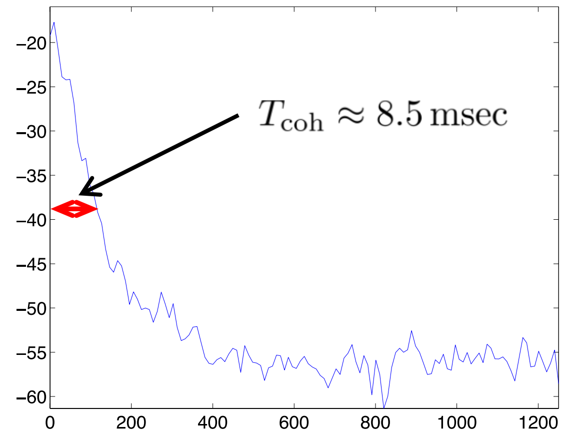

- We simplify fading to a two-parameter model $\{\sigma_l^2, T_{\text{coh}}\}$

lognormal fading variance

coherence time

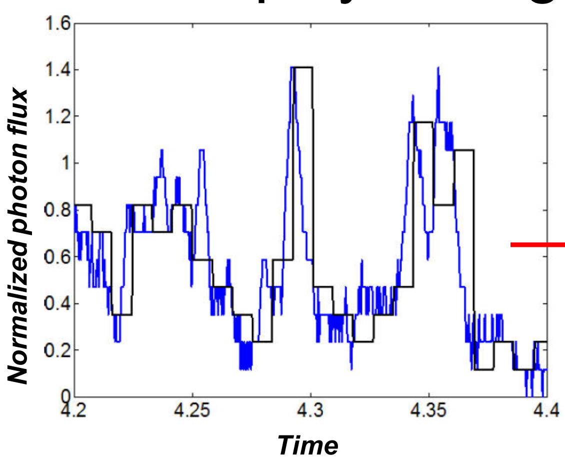

Model fades as drawn independently from a log-normal distribution every T_{coh} seconds, and constant over those intervals.

Mitigating outages with interleaving

- Codewords are significantly shorter than the rate of photon-flux fluctuations
  - with no mitigation there is always a finite probability of a fade deep enough to corrupt a codeword $\Rightarrow$ unconditional reliability not possible

- To assure reliability, each codeword should see a 'well-mixed' channel
  - interleaving achieves this goal, as $N \to \infty$ rate of reliable transmission converges to ergodic capacity $C_{\mathrm{E}}(\sigma_I^2, T_{\mathrm{coh}}) \equiv \langle C(P_0, V) \rangle_V$

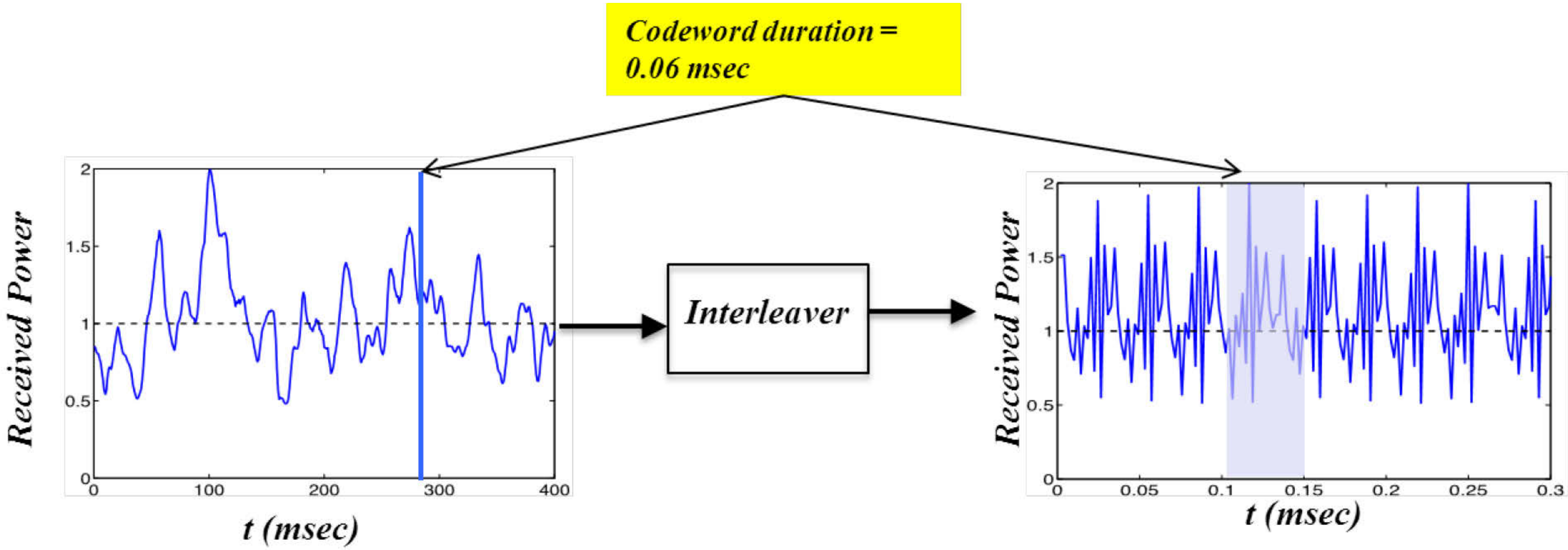

Capacity loss due to fading

- We have $C_{\mathrm{E}}(P_0, \sigma_I^2, T_{\mathrm{coh}}) \leq C_E(P_0, 0, \infty)$
  - fading dynamics cause *unrecoverable* loss at equal mean photon flux

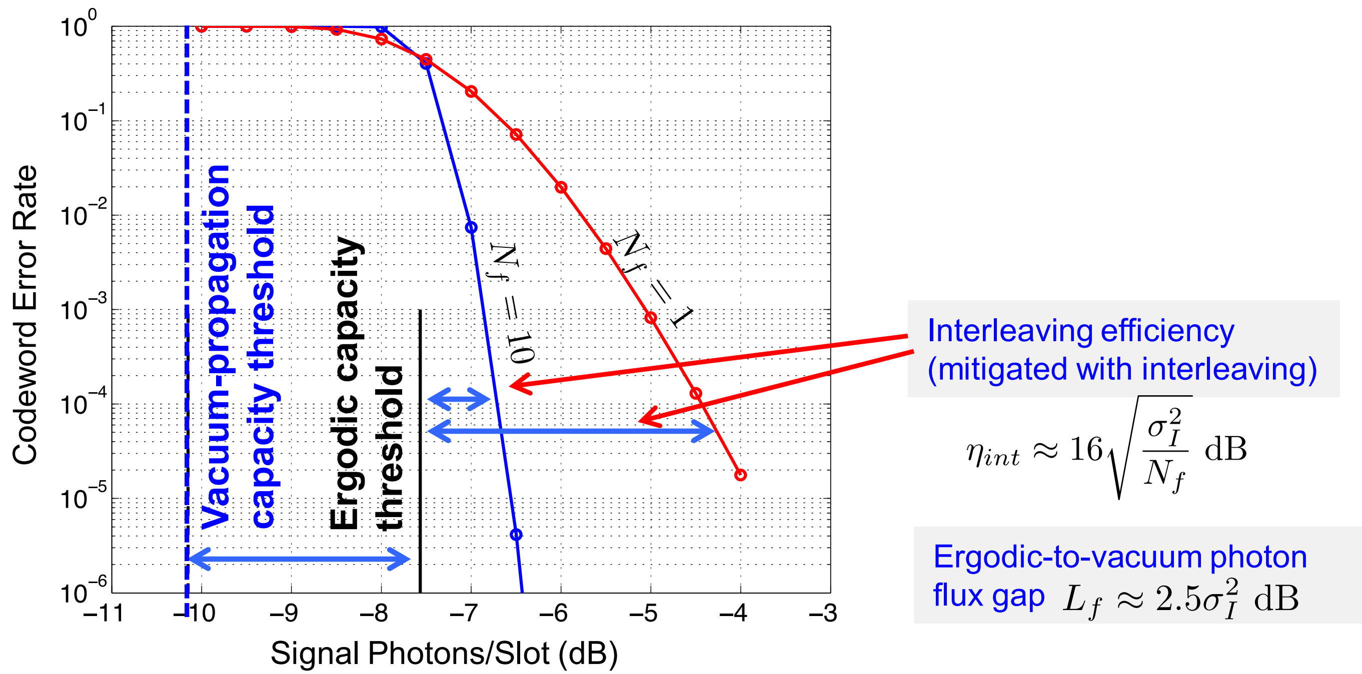

- Finite-depth interleaving ($N < \infty$) results in a nonzero outage probability and an increase in required power

Channel impairments

II. Pointing effects

Transmitter-induced pointing errors

- Transmitter often performs active tracking on beacon (or received communication beam in bidirectional links) to minimize pointing errors

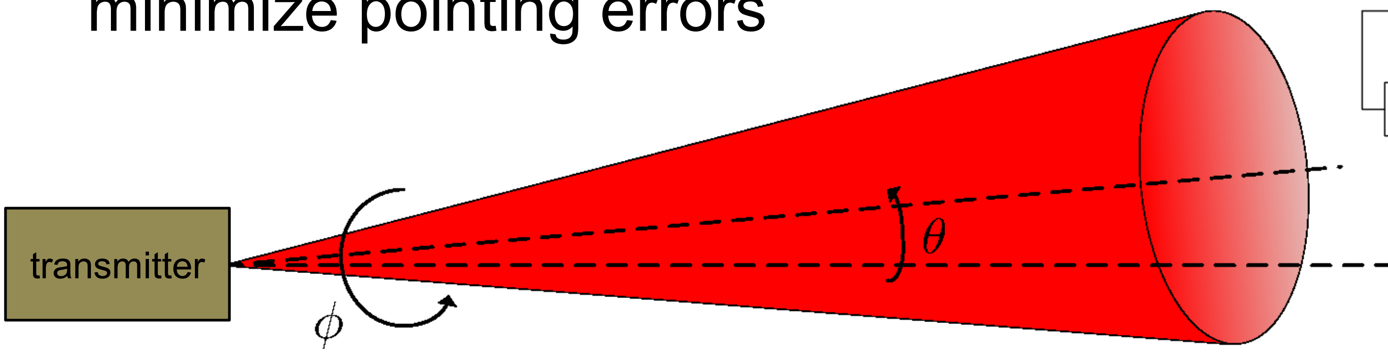

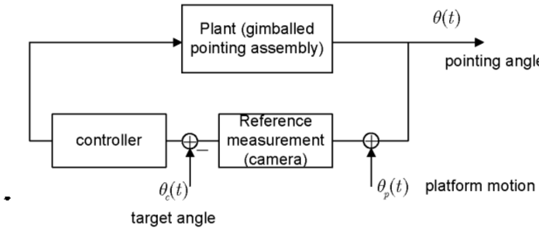

- Assuming a circularly-symmetric Gaussian beam, and a Gaussian random process for $\theta(t)$

pointing-error variance

marginal probability distribution (averaged over a uniform ϕ):

$$p(\theta) = \frac{\theta}{\sigma^2} e^{-(\theta_m^2+\theta^2)/(2\sigma^2)} I_0\left(\theta_m \theta / \sigma^2\right)$$

mean pointing error

- Impact on link is similar to that of turbulence-induced fades

$$P_r(t) = P_0 B_G\left(\theta(t)\right)$$

on-axis irradiance

normalized beam profile

Receiver-induced pointing errors

- The telescope can be thought of as a *big* aperture and an effective lens focusing the incoming light on a photodetector
- If telescope is off-pointed by θ relative to optical axis, the beam will focus off-center

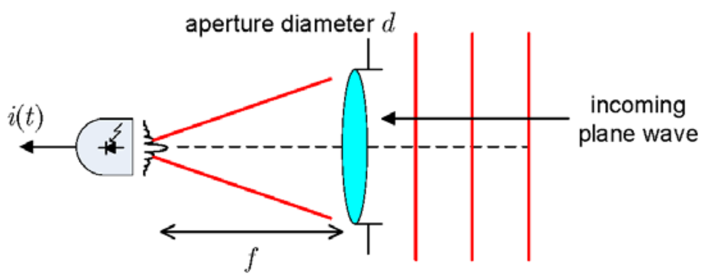

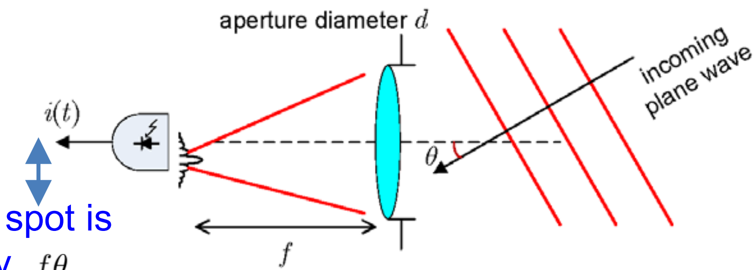

translation of spot is approximately $f\theta$

- The long-exposure image integrates over many jitter-induced translations, resulting in broadened spot
  – The average pulse approaches Gaussian as exposure time increases and has *approximate width* $f\sqrt{\theta_{\mathrm{rms}}^2 + (\frac{a\lambda}{D})^2}$ (a is some constant)
- Impact is similar to that of angle-of-arrival spread

Channel impairments
III. Receiver effects

Background radiance

- The receiver collects background light along with signal
  - scattered sunlight (daytime)
  - light from point sources in field-of-view (both daytime and nighttime)
- Background light is treated as uniform incoherent illumination on the photodetector

Sky Radiance

$$P_n = B_\lambda \times A_R \times \Omega \times \Delta\lambda \times \eta_R$$

Aperture area | Field-of-View | Bandwidth | Efficiency

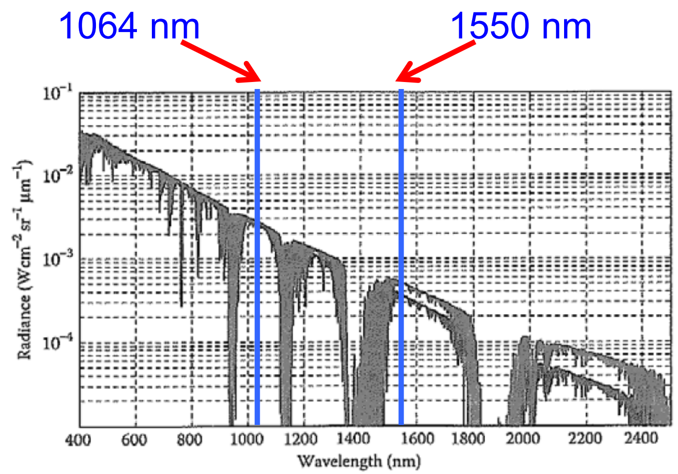

FIGURE 8.16 Daytime sky radiance at 2 km above sea level. The Sun zenith angle is 45°. Two cases (radiance curves) are shown: (1) the observer zenith angle on the ground is at 40° (higher radiance curve) and (2) the observer zenith angle on the ground is at 70° (lower radiance curve). The rural aerosol model with a visibility of 23 km at sea level was used. Data obtained after MODTRAN simulation.

Piazzolla, Near-Earth Laser Communications 2009

Efficiency trade-off with finite background

- K background noise modes (*iid*, complex-Gaussian amplitude distribution), N counts/mode

$$p_1(k;K) = \frac{N^k}{(1+N)^{k+K}} L_k^{(K-1)}\left(\frac{-n_s}{N(1+N)}\right) e^{-n_s/(1+N)}$$

Negative binomial distribution

$$p_1(n;K) \xrightarrow[K\to\infty]{} \frac{(n_b+n_s)^n e^{-(n_b+n_s)}}{n!}$$

Poisson approximation

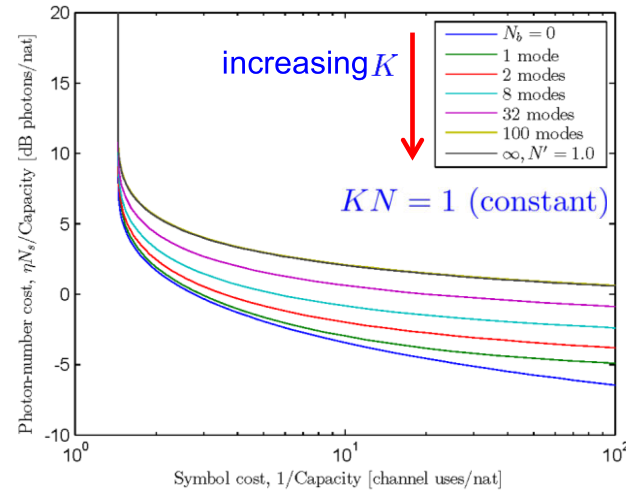

- Thermal noise bounds photon efficiency

$$c_p^{\mathrm{Hol}}(n_b) \le \log_2(1 + 1/n_b) \qquad (n_b \equiv KN)$$

- Poisson approximation gives unbounded photon efficiency
  - Poisson approximation to multimode thermal noise must become inaccurate at large c_p for any number of noise modes

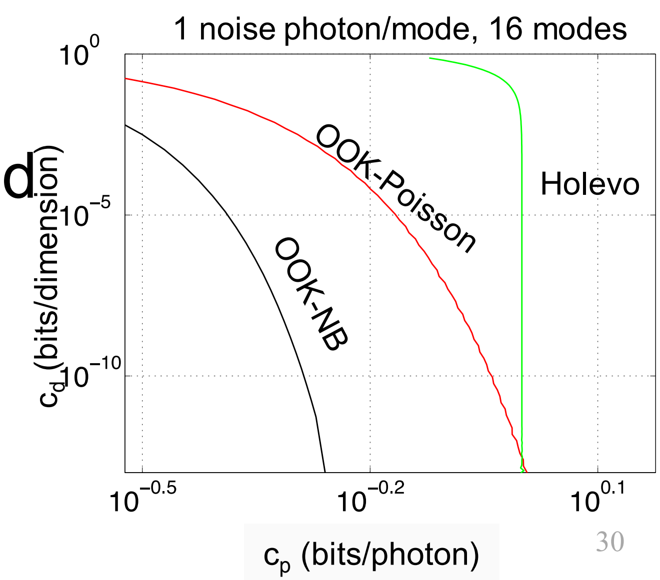

Dark noise of photodetector

- *Dark noise* is spurious photoelectrons that are generated even with no incident light
  - dark current is a Poisson-distributed signal-independent background noise n_b.

$$n_d = \ell_d A T_s \quad \text{dark e/slot}$$

surface dark rate

active area

slot width

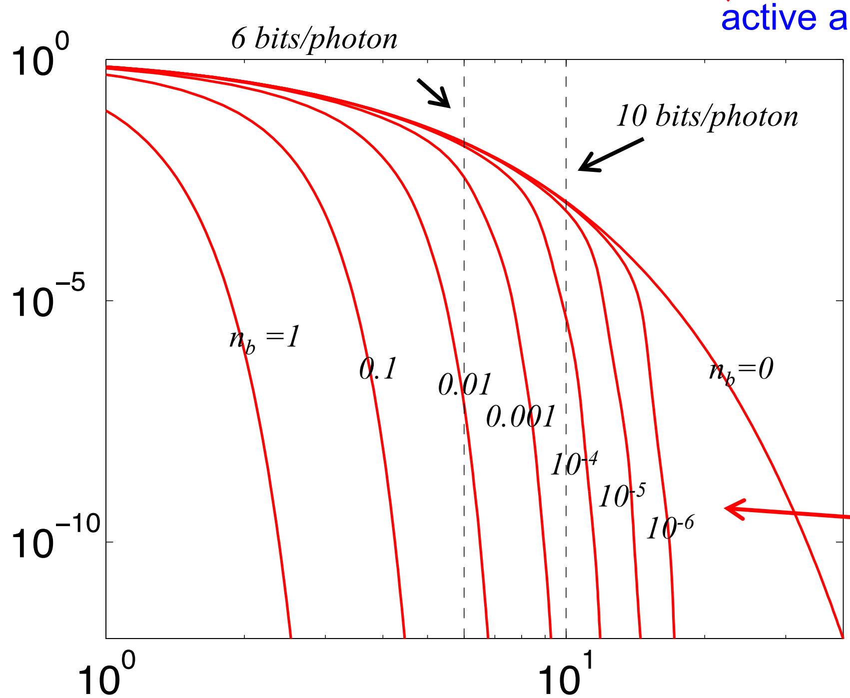

Device	ℓ_d (e/s/mm²)
Si GM-APD	10^6
InGaAsP GM-APD	10^8
NbN SNSPD	10^2

Noise levels with $n_b > 10^{-5}$ incur large losses beyond 10 bits/photon.

Efficiency trade-off with finite dark noise

- The photon-efficiency of OOK + photon-counting is effectively bounded because spectral efficiency drops off doubly-exponentially: $c_d < \beta c_p 2^{-\beta c_p}$ $\quad \beta = \max(1, e n_b 2^{c_p})$
  - this approximate bound crosses the noiseless OOK and Holevo curves at

$$c_p \approx \log_2 \left(\frac{1}{e n_b} \right)$$

  - The actual c_d breaks away sharply from the noiseless OOK curve when $M n_b \approx 1/e^4 = 0.018$ noise counts/PPM symbol

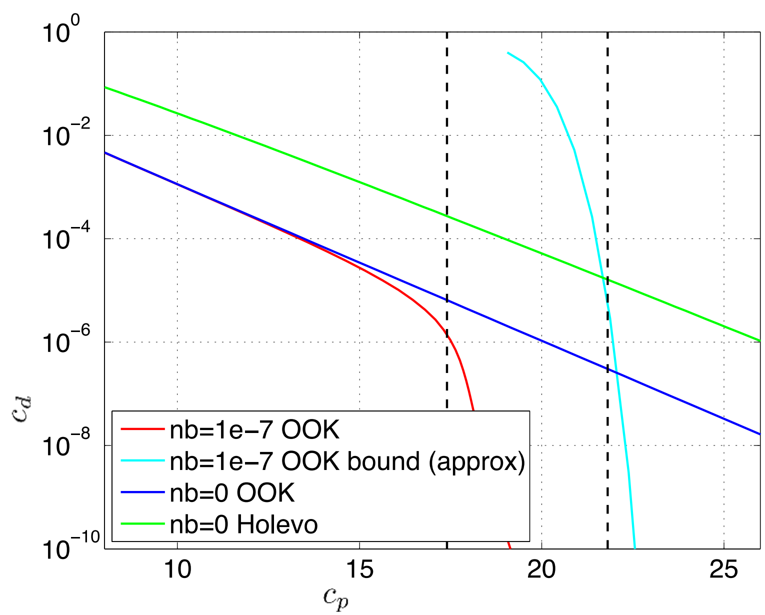

Finite extinction ratio of laser transmitter

- Non-ideal lasers 'leak' some power in the *off* state:
  - leaked power is proportional to power in the *on* state; the proportionality constant is the extinction ratio α.

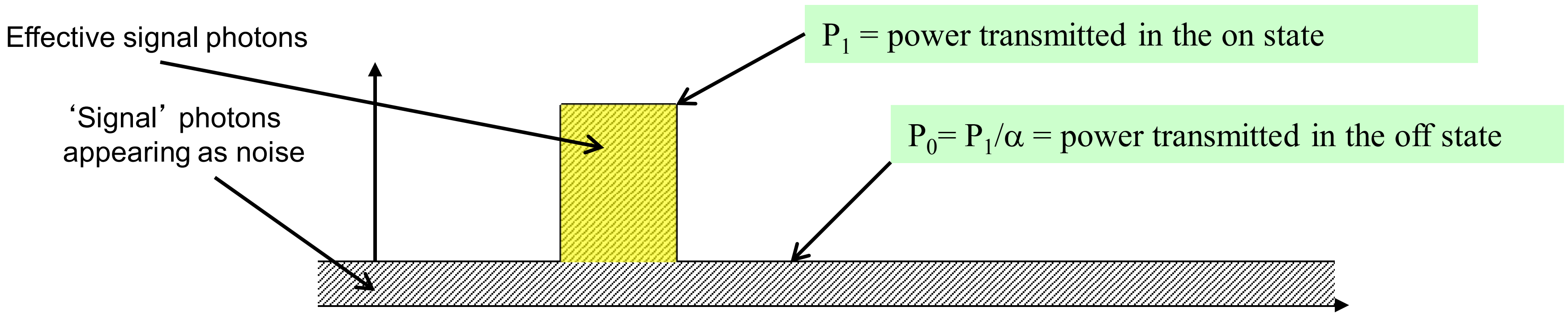

- generates a Poisson-distributed background noise proportional to the signal $n_b = n_s/\alpha$

- With finite extinction ratio α, the photon efficiency of OOK + photon counting is strictly bounded:

$$c_p \lessapprox \log_2(\alpha) - 1/\ln(2) \text{ (bits/effective signal photon)}$$

Efficiency trade-off with finite extinction ratio

- Each curve in these plots is the capacity efficiency tradeoff for a given PPM order *M*, and is generated by varying the average number of signal photons.

No dark noise

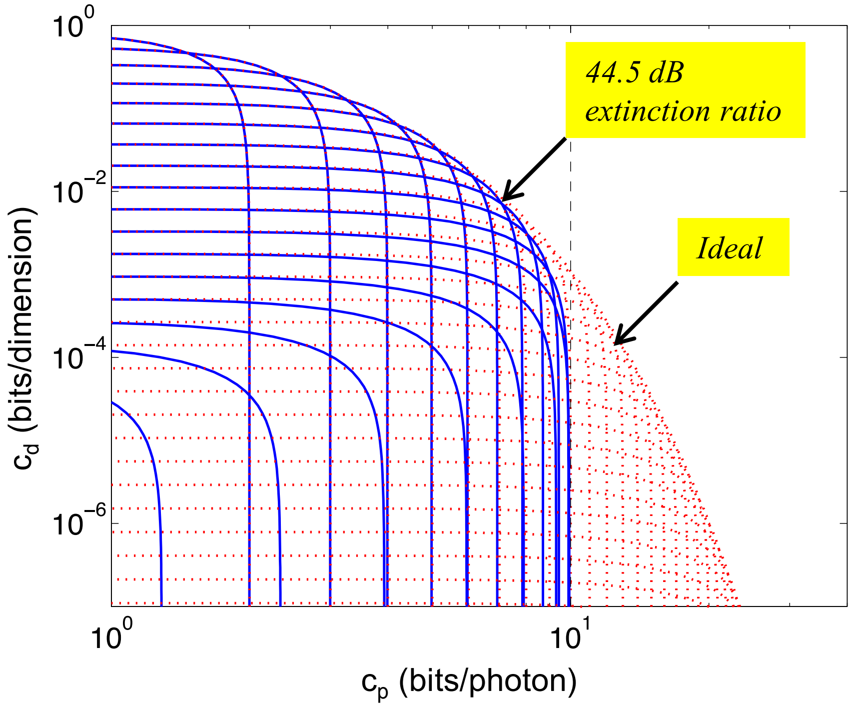

Dark noise rate 10^{-6} e/slot
(e.g., 1 kHz dark rate, 1 ns slot)

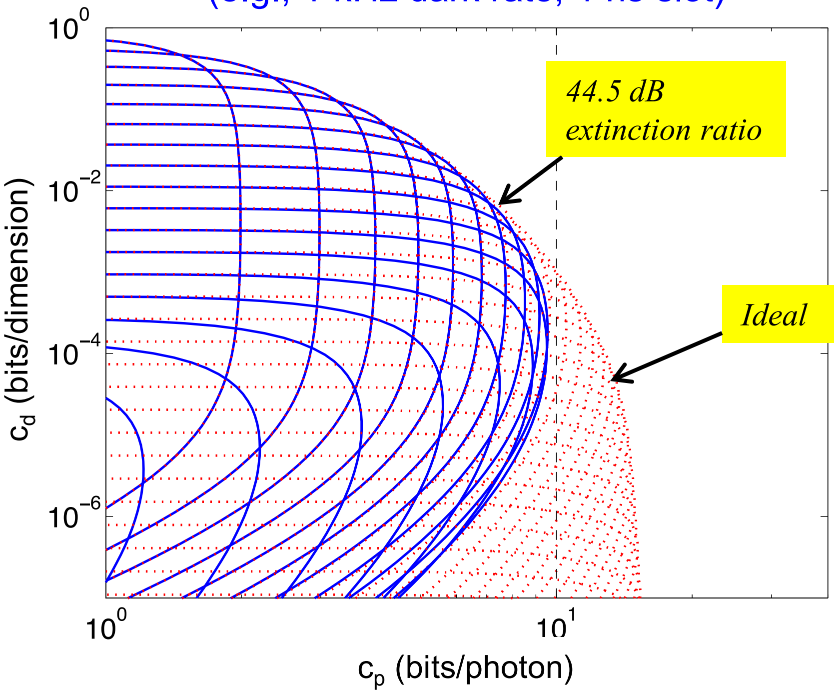

Timing jitter at the photodetector

- Jitter is the *random delay* from the time a photon is incident on a photo-detector to the time a photo-electron is detected

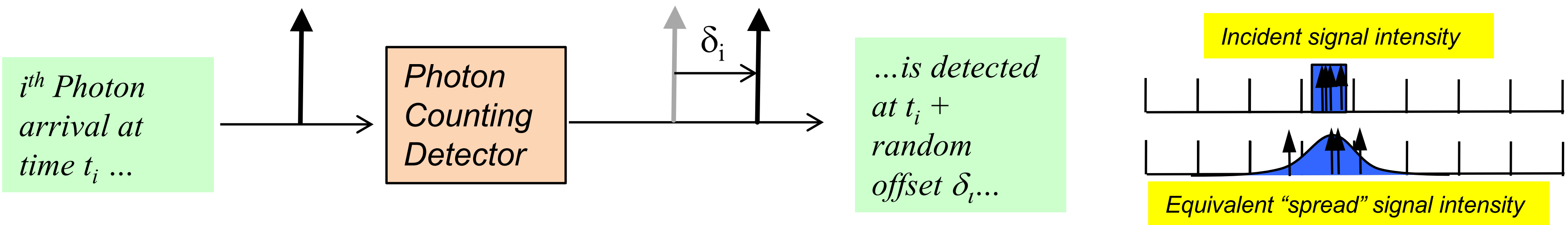

- Jitter losses are a function of the *normalized jitter standard deviation*: σ_j / T_s

jitter standard deviation

Slot-width

- Losses grow rapidly when $\sigma_j / T_s > 0.1$

Device	σ / 1ns
InGaAs(P) PMT	0.9
InGaAs(P) GM-APD	0.3
Si GM-APD	0.24
NbN SNSPD	0.03

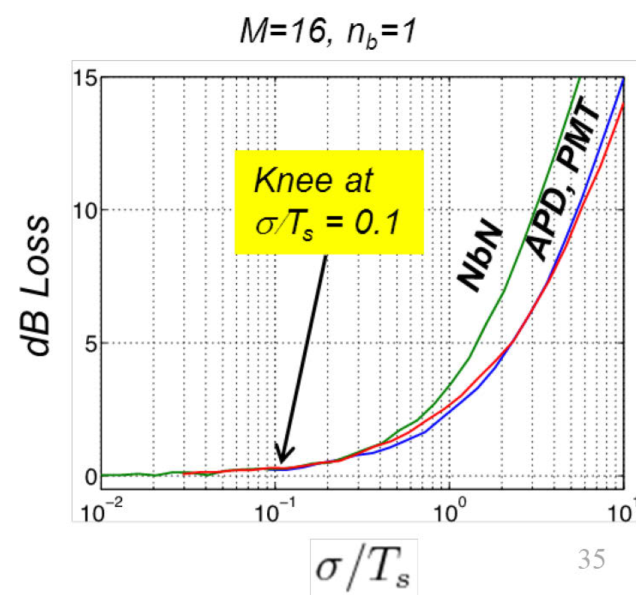

Photodetector blocking

- Photon-counting detectors are rendered inoperative (**blocked**) for some time τ (**dead time**) after each detection
  - 10-50 ns for SiGM-APD
  - 1-10 μs for InGaAs GM-APD
  - 3-20 ns, for NbN SNSPD
- Blocking can be modeled as a Markov chain

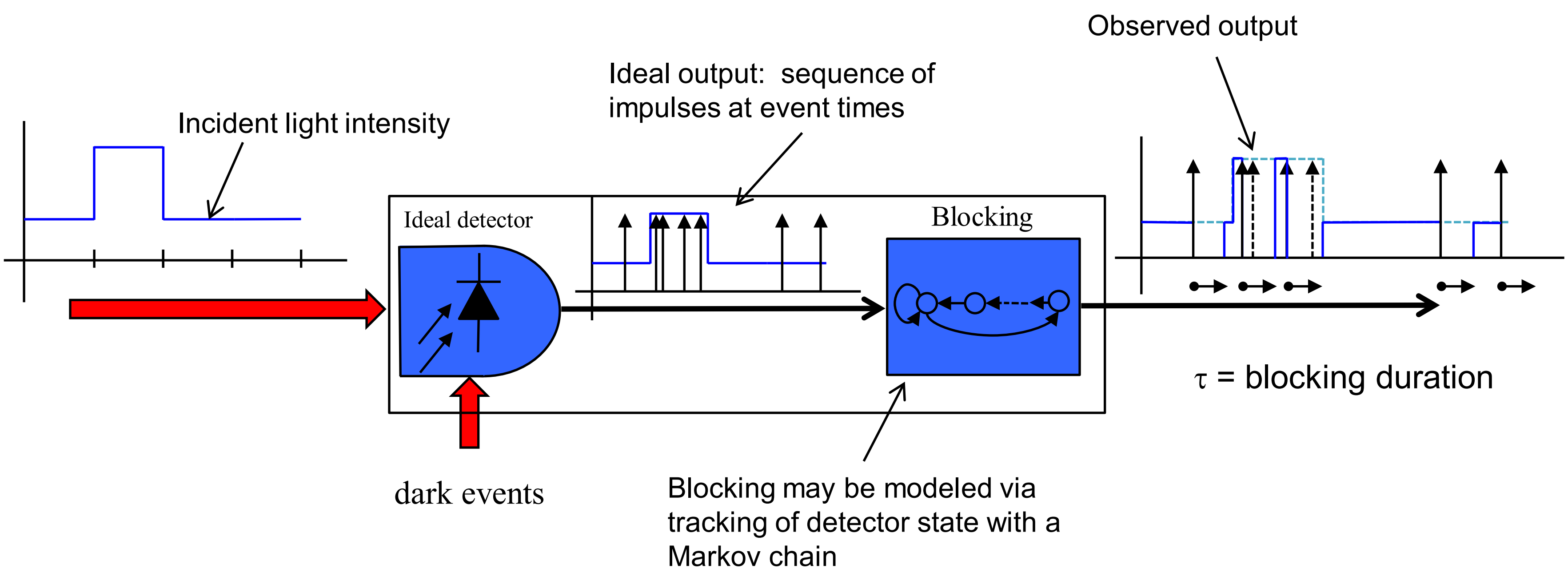

Mitigating blocking

- Blocking may be mitigated by decreasing the peak incident photon rate (per detector)
- *Temporal*: Increase slot-width and reduce photon rate, while preserving photons/slot
  - lowers date rate, and integrates more noise

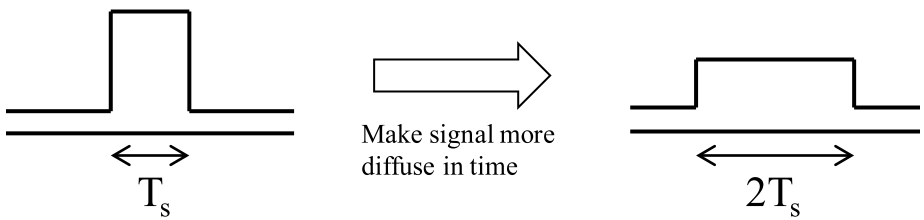

- *Spatial*: Increase focal length, and illuminate photodetector array instead of single photodetector
  - integrates more noise from multiple pixels

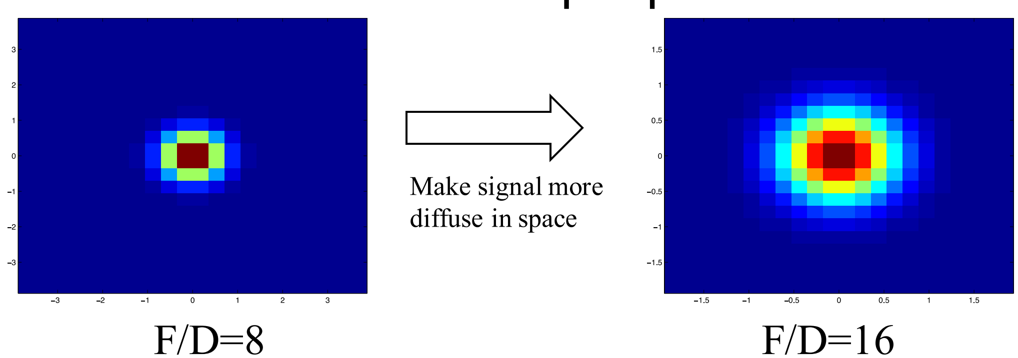

Quantifying blocking loss

- Model blocking by splitting time into small time bins, and modeling the blockage as a Markov chain

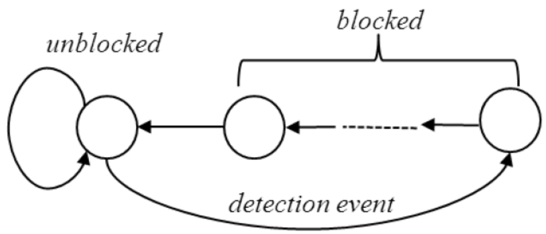

$$\mu \approx \frac{1}{1+\tau l}$$

μ = steady-state probability of unblocked state

ℓ =incident photon rate

- Approximate the photodetector output as a Poisson process

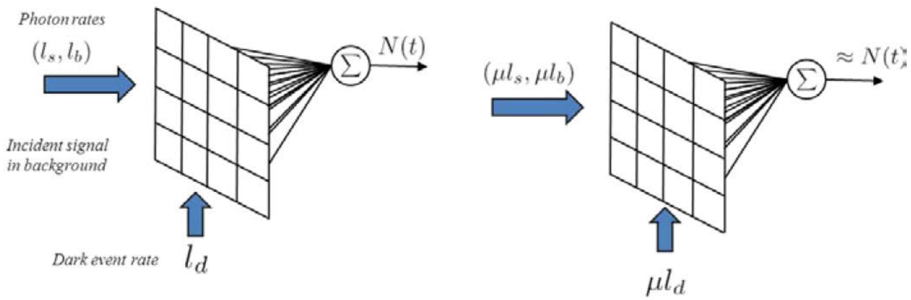

- Signal Power Loss: increase in power to achieve fixed capacity

$$C_b(l_s') = C_u(l_s)$$

$$\frac{l_s}{l_s'} \approx \begin{cases} \mu & high\ SNR \\ \sqrt{\mu} & low\ SNR \end{cases}$$

- Capacity Loss: decrease in capacity at fixed signal power $\frac{C_b}{C_u} = \mu$

Putting it back together

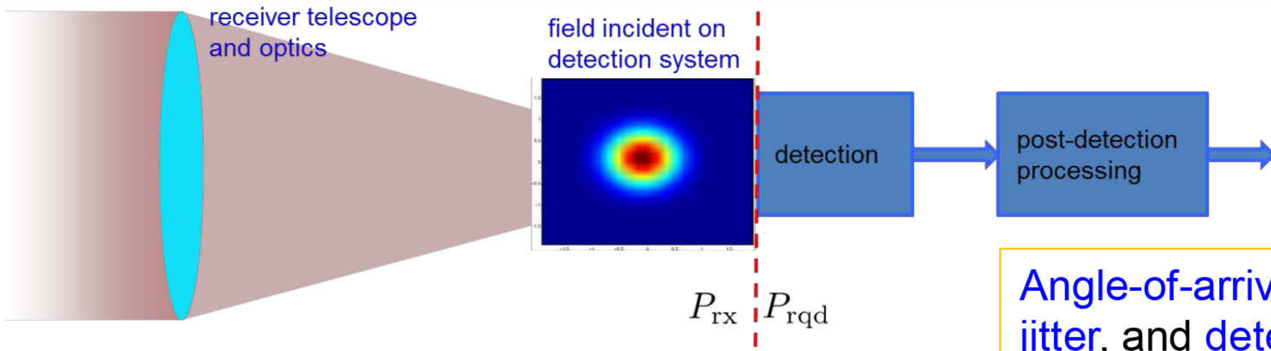

Angle-of-arrival spread, receiver pointing jitter, and detector blocking are mitigated by increasing the field-of-view of receiver, but dark noise and background radiance are traded to find optimum

Extinction ratio loss is mitigated with better engineered sources

$$P_{\mathrm{rx}} = P_t G_t G_r L_s L_a \eta_{\mathrm{pt}} \eta_t \eta_r$$

$$P_{\mathrm{rqd}} = P_i / (L_b L_j L_f L_t \eta_{\mathrm{det}} \eta_{\mathrm{imp}} \eta_{\mathrm{code}} \eta_{\mathrm{int}})$$

Photon-flux fluctuations caused by atmospheric turbulence and pointing errors are mitigated by *interleaving* the data

Detector temporal jitter is mitigated by utilizing slots that are wide enough

Conclusions

- Free-space optical communication systems potentially gain many dBs over RF systems
- Deep-space optical communication links are *photon-starved*
  - presently binary intensity modulation + photon-counting is best known technique to achieve high photon efficiency
- Reliable information transmission requires both physical and link layer engineering:
  - active tracking systems are employed to maintain as stable and robust a line-of-sight as possible
  - Error-correction coding is employed to ensure reliability in the presence of errors
- Receiver noises, detector losses, pointing errors, and atmospheric effects must all be accounted for:
  - Theoretical models are used to analyze performance degradations
  - Mitigation strategies derived from this analysis are applied to minimize these degradations